

# Quantum entanglement in photosynthetic light harvesting complexes

Mohan Sarovar,<sup>1,2,\*</sup> Akihito Ishizaki,<sup>2,3</sup> Graham R. Fleming,<sup>2,3</sup> and K. Birgitta Whaley<sup>1,2</sup>

<sup>1</sup>*Berkeley Center for Quantum Information and Computation, Berkeley, California 94720 USA*

<sup>2</sup>*Department of Chemistry, University of California, Berkeley, California 94720 USA*

<sup>3</sup>*Physical Bioscience Division, Lawrence Berkeley National Laboratory, Berkeley, California 94720 USA*

Light harvesting components of photosynthetic organisms are complex, coupled, many-body quantum systems, in which electronic coherence has recently been shown to survive for relatively long time scales despite the decohering effects of their environments. Within this context, we critically analyze entanglement in multi-chromophoric light harvesting complexes; we clarify the connection between coherence and entanglement in these systems, and establish methods for quantification of entanglement by presenting necessary and sufficient conditions for entanglement and by deriving a measure of global entanglement. These methods are then applied to the Fenna-Matthews-Olson (FMO) protein to extract the initial state and temperature dependencies of entanglement in this complex. We show that while FMO in natural conditions largely contains bipartite entanglement between dimerized chromophores, a small amount of long-range and multipartite entanglement exists even at physiological temperatures. This constitutes the first rigorous quantification of entanglement in a biological system. Finally, we discuss the practical utilization of entanglement in densely packed molecular aggregates such as light harvesting complexes.

## I. INTRODUCTION

Unlike in classical physics, within quantum mechanics one can have maximal knowledge of a composite physical system and still not be able to assign a definite state to its constituent elements without reference to their relation to each other [1, 2]. Such systems are called entangled, and entanglement is a characteristic quantum mechanical effect that has been widely investigated in recent years [3, 4]. Entanglement is often viewed as a fragile and exotic property, and in the quantum information context, where it is used as a resource for information processing tasks, precisely engineered entangled states of interest can indeed be both fragile and difficult to manufacture. However, it has also been recognized that entanglement is a natural feature of coherent evolution, and recently, there has been an effort to expand the realms in which entanglement can be shown to exist rigorously, particularly in “natural” systems – i.e., not ones manufactured in laboratory conditions. Signatures of entanglement, a characteristically quantum feature, have been demonstrated in thermal states of bulk systems at low temperatures and between parties at macroscopic length scales [5]. Additionally, several recent studies have focused on the dynamics of entanglement in damped, driven, or generally non-equilibrium quantum systems [6, 7, 8]. The dynamics of entanglement in open systems can be extremely non-trivial – especially in many-body systems – and the precise influence of non-Hamiltonian dynamics on entanglement is poorly understood. In a result particularly relevant to this work, it is shown in Ref. [8] that entanglement can be continuously generated and destroyed by non-equilibrium effects in an environment where no static entanglement exists. The possibility of

entanglement in noisy non-equilibrium systems at high temperatures intimates the question: can we observe entanglement in the complex non-equilibrium chemical and biological processes necessary for life? Here we present strong evidence for answering this question in the affirmative by determining the timescales and temperatures for which entanglement is observable in a protein structure that is central to photosynthesis by green anoxygenic bacteria.

Recent ultrafast spectroscopic studies have revealed the presence of quantum coherence at picosecond timescales in biological and molecular structures [9, 10, 11]. These studies demonstrate that in moderately strongly coupled, non-equilibrium systems, quantum features can be observed even in the presence of a poorly controlled, decohering environment. Light harvesting complexes – the densely packed molecular structures involved in the initial stages of photosynthesis – have been the subject of many of these spectroscopic studies, and much is known about their structural and dynamical properties. In this paper we formulate conditions and measures of entanglement in light harvesting complexes. We demonstrate that entanglement can realistically be observed in such systems by constructing a simple and experimentally amenable entanglement witness for the Fenna-Matthews-Olson (FMO) light harvesting complex (LHC) and predicting through realistic simulations of FMO dynamics that entanglement will be present in the structure at observable timescales. We fully characterize the degree and dynamics of entanglement in the FMO complex for several realistic initial states and environmental conditions. We further comment on the role of entanglement in the functioning of light harvesting complexes and discuss applications of entanglement in such systems.

---

\*Electronic address: msarovar@berkeley.edu

## II. LIGHT HARVESTING COMPLEXES AND ENTANGLEMENT

During the initial stage of photosynthesis, light is captured by pigment-protein antennas, known as light harvesting complexes, and the excitation energy is then transferred through these antennas to reaction centers (RC) where photosynthetic chemical reactions are initiated. There are several varieties of LHCs. These differ in their detailed structure, but all consist of densely packed units of pigment molecules and all are spectacularly efficient at transporting excitation energy in disordered environments [12]. The number of chromophores (pigments) and the average inter-chromophore distance varies between LHCs, but separations on the scale of  $\sim 15\text{\AA}$  are fairly common. At these distances, the dipole coupling of these chromophoric molecules is considerable and leads to coherent interactions at observable timescales. The presence of this “site” coherence (coherence between spatially separated pigment molecules) has been recognized for some time [13, 14]. It is this site coherence that prompts us to examine entanglement in these systems and to consider the timescales and temperatures at which entanglement can exist.

We begin by noting that in natural conditions the majority of LHCs contain at most one excitation at any given time. This is especially true of light harvesting complexes in photosynthetic bacteria (which are among the ones most heavily studied) because these bacteria receive very little sunlight in their natural habitat. Given this, we can think of each chromophore as a two-level system, and the general state of an LHC is then specified in this single-excitation manifold as:

$$\rho(t) = \sum_{i=1}^N \rho_{ii}(t) |i\rangle\langle i| + \sum_{i=1}^N \sum_{j>i}^N \rho_{ij}(t) |i\rangle\langle j| + \rho_{ij}^*(t) |j\rangle\langle i| \quad (1)$$

where  $|i\rangle$  represents the state where only the  $i$ th chromophore (site) is excited and all other chromophores are in their electronic ground states – e.g.  $|2\rangle \equiv |0\rangle \otimes |1\rangle \otimes |0\rangle^{\otimes N-2}$ . This representation of the state is in what is usually referred to as the *site basis*. Within the single excitation manifold, the density matrix has dimension  $N \times N$ , where  $N$  is the number of chromophores in the LHC.

Electronic excitation dynamics is governed by a Hamiltonian of the form:  $H = H_{\text{el}} + H_{\text{el-env}} + H_{\text{env}}$ , where

$$H_{\text{el}} = \sum_{i=1}^N E_i |i\rangle\langle i| + \sum_{i=1}^N \sum_{j>i}^N J_{ij} (|i\rangle\langle j| + |j\rangle\langle i|) \quad (2)$$

describes the closed system dynamics of the  $N$  LHC chromophores, including on-site energies,  $E_j$ , and coupling terms,  $J_{ij}$ , that describe the dipole coupling of the chromophores. The remaining terms in  $H$  describe the coupling between the electronic degrees of freedom of the LHC chromophore molecules and their environment, which typically consists of surrounding proteins,

the electromagnetic field, and reaction center/s that the LHC is affixed to. An accurate reduced description of the effective dynamics of the excitation state  $\rho$  will depend on the explicit details of the environment and its coupling to the LHC. However, in general the environmental coupling terms lead to dephasing and dissipation of the excitation state  $\rho$ . Because of this, we will treat  $\rho$  as an unnormalized density matrix from hereonwards – that is,  $\sum_i \rho_{ii}(t) \neq 1$ , because the single excitation state has a finite lifetime due to trapping by the reaction center complex and spontaneous emission.

Given an unnormalized density matrix  $\rho$  representing a single excitation state, we wish to calculate the amount of entanglement in the state. Note that entanglement in the site basis refers to non-local correlations between the electronic states of spatially separated chromophores. Mixed-state, multi-partite entanglement is notoriously difficult to quantify [3], but we will use the single-excitation restriction to formulate a useful measure. First, note that if  $\rho$  represents a single excitation state, we have the following:

**Proposition 1:**  $\rho$  entangled  $\iff \rho_{ij} \neq 0$  for some  $i \neq j$ .

Here, the right hand side simply means that  $\rho$  has some coherence. Hence, coherence (in the site basis) in the single excitation subspace is necessary and sufficient for entanglement.

**Proof:** The forward implication is clearly seen from its contrapositive form:  $\rho_{ij} = 0 \ \forall i \neq j \implies \rho$  separable. If  $\rho_{ij} = 0 \ \forall i \neq j$ , then the state has the form  $\rho = \sum_i \rho_{ii} |i\rangle\langle i|$ , which is clearly a separable state since each  $|i\rangle$  is separable. To prove the backward implication, again consider its contrapositive form:  $\rho$  separable  $\implies \rho_{ij} = 0 \ \forall i \neq j$ . If  $\rho$  is separable it contains no entanglement, and specifically no bipartite entanglement between any two chromophores. The well known mixed state bipartite entanglement measure for two-level systems, *concurrence* [15], can be computed between chromophores 1 and 2. In the single excitation subspace, it evaluates to  $C_{12} = 2|\rho_{12}|$ . Hence, zero bipartite entanglement between these chromophores implies  $\rho_{12} = 0$ . Similarly, by setting the bipartite entanglement between all pairs of chromophores to zero, we find that  $\rho_{ij} = 0 \ \forall i \neq j$ . ■

This property of states in the single excitation subspace means that an effective entanglement witness [16, 17] for these states is simply the sum of all coherences:

$$\mathcal{W} = \sum_{i<j} |\rho_{ij}| \quad (3)$$

That is,  $\mathcal{W} > 0 \iff \rho$  entangled. Note that unlike most entanglement witnesses, which only present sufficient conditions for entanglement, in this case  $\mathcal{W} > 0$  is both necessary and sufficient for entanglement. Practically this property can therefore be used in experiments to detect entanglement; any non-zero off-diagonal component of the LHC single excitation density matrix in the site basis is a signature of entanglement. Simplifica-

tions of this witness, which become sufficient conditions for entanglement, can also be formulated by restricting the sum to be over a subset of the off-diagonal elements – this could be useful in situations where accessing all off-diagonal elements is experimentally prohibitive.

Lastly, we can proceed further and also construct a measure of global entanglement in this system. A strict entanglement measure is non-increasing under local operations and classical communications and invariant under local unitaries [3]. A particularly useful such measure for characterizing multipartite entanglement in single excitation LHC states is the *relative entropy of entanglement* [18]. This measure of entanglement for a state  $\rho$  is:

$$E[\rho] = \min_{\sigma \in \mathcal{S}} S(\rho||\sigma) \quad (4)$$

where  $\mathcal{S}$  is the set of separable states and  $S$  is the relative entropy function:  $S(\rho||\sigma) = \text{tr}(\rho \ln \rho - \rho \ln \sigma)$ . Physically,  $E$  quantifies the entanglement in  $\rho$  as the distance between  $\rho$  and the closest separable state to it, where the distance measure is based on the asymptotic distinguishability of two states [19]. In our case, we know from *Proposition 1* above that the set of separable states have diagonal form and hence the minimization problem becomes:

$$\begin{aligned} E[\rho] &= \min_{p_i} \text{tr}(\rho \ln \rho - \rho \ln \sigma) \\ \text{subject to} & \sum_{i=1}^N p_i = \text{tr} \rho \end{aligned} \quad (5)$$

where  $\sigma = \text{diag}(p_1, p_2, \dots, p_N)$ , and the optimization constraint comes from the fact that we are only considering separable states with the same normalization as  $\rho$ . The cost function is convex in  $p_i$  and the constraint is linear so this optimization is easily solved (e.g. by using a Lagrange multiplier to combine the cost function and constraint into a Lagrangian and then finding its stationary point) to obtain an expression for the closest separable state:  $\sigma^* = \text{diag}(p_1^*, p_2^*, \dots, p_N^*)$  with  $p_i^* = \rho_{ii}$ , and also a measure of global entanglement in the state  $\rho$ ,

$$E[\rho] = - \sum_{i=1}^N \rho_{ii} \ln \rho_{ii} - S(\rho). \quad (6)$$

Here  $S(\rho) = -\text{tr} \rho \ln \rho$  is the von Neumann entropy of the state  $\rho$ . Consistent with our discussion above,  $E[\rho]$  is also a measure of coherence in the system since the first quantity in the expression is the entropy of a state with all the coherences in  $\rho$  set to zero.

In the following section we will use these characterizations of entanglement in LHCs together with realistic simulations to make predictions about entanglement in the Fenna-Matthews-Olson photosynthetic complex, including initial state and temperature dependence.

### III. ENTANGLEMENT DYNAMICS IN THE FMO COMPLEX

A commonly studied LHC is the Fenna-Matthews-Olson (FMO) protein from green sulfur bacteria, such as *Chlorobium tepidum* [20, 21]. The FMO complex is a trimer formed by three identical monomers that each bind seven bacteriochlorophyll-*a* (BChl*a*) molecules. We will restrict our study to a single monomer, which is shown in Fig. 1, since it is believed that the monomers function independently. The site energies of the BChl*a* molecules and coupling between molecules are well characterized; we use the *Chlorobium tepidum* site energies and coupling strengths from table 4 (the trimer column) and table 1 (column (4)) of Ref. [22] to form a Hamiltonian that describes the closed-system dynamics of an FMO monomer. The structure of the Hamiltonian indicates that some pairs of chromophores are moderately strongly coupled (due to their close proximity and favorable dipole orientations) and hence effectively form *dimers*. The wavefunctions of the system’s energy eigenstates, usually called *Frenkel excitons*, are primarily delocalized across these dimers. The dominant dimers are formed by chromophore pairs: 1-2, 5-6, and 3-4.

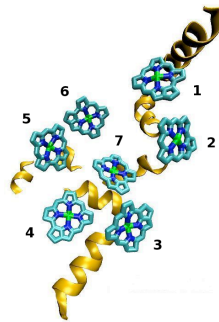


FIG. 1: Schematic of a Fenna-Matthews-Olson complex monomer. The multiring units are bacteriochlorophyll-*a* (BChl*a*) molecules and the spiral strands are  $\alpha$ -helices that are part of the protein environment in which the BChl*a* molecules are embedded. The numbers label individual BChl*a* molecules, also referred to as “sites” in the main text. The incoming excitations are received by sites 1 and 6, and the reaction center is selectively coupled to site 3.

In addition to the closed-system (Hamiltonian) dynamics of the seven BChl*a* chromophores in an FMO monomer, there are interactions between each chromophore and the protein environment that it is embedded in. These interactions couple the protein dynamics to the FMO energy levels, resulting in static and dynamic disorder, and thereby lead to dephasing of the FMO electronic excitation state. Coherence properties of the FMO protein are then dictated by the interplay between coherent dynamics of the complex and decoherence effects due to environmental interactions. Distinctly quantum properties such as entanglement rely critically on coherence and therefore it is essential that a model that accurately

accounts for environmental effects on coherence be used to make predictions about entanglement in FMO.

Quantum master equation approaches are commonly used to explore the dynamics of photosynthetic excitation energy transfer (EET), particularly the standard Redfield equation [23, 24]. This equation is valid when the interchromophoric coupling is much smaller than the electron-phonon coupling – which can be specified by the magnitude of the reorganization – because the equation is derived on the basis of a second-order perturbative truncation with respect to the electron-phonon coupling. However, in the FMO complex the reorganization energies are not small in comparison to the interchromophoric coupling: the electronic coupling strengths span a wide range,  $1 \sim 100 \text{ cm}^{-1}$ , and the typical reorganization energies span a similar range [22, 25, 26, 27]. Hence, the standard Redfield equation approach might lead to erroneous insights and incorrect conclusions regarding quantum coherent effects in the FMO complex [28]. Recently, Ishizaki and Fleming have developed a nonperturbative quantum master equation for photosynthetic EET that takes into account the phonon relaxation dynamics associated with each chromophore in chromophore-protein complexes [29, 30]. This results in a set of hierarchically coupled equations for the reduced density matrix that can describe quantum coherent wave-like motion and incoherent hopping motion in a unified manner, and which reduces to the standard Redfield theory and Förster theory [24, 31] in their respective limits of validity. In the following we characterize entanglement in FMO by simulating the evolution of excitation energy in the FMO monomer using this recently formulated model of photosynthetic EET that incorporates the dynamics of phonon reorganization in a realistic manner. For all the simulations below we assume that the reorganization energy of the molecular environment is  $35 \text{ cm}^{-1}$ , a value that is consistent with experimentally observed and theoretically calculated reorganization energies for this complex [22, 25, 26, 27]. In addition, we use a phonon relaxation time of 100fs, and a reaction center trapping rate associated with site 3 of  $(4 \text{ ps})^{-1}$ , both of which are consistent with the literature on FMO [22, 26].

Due to FMO energy levels and physical structure, it is believed that sites 1 and 6 interface with the light energy providing chlorosome and therefore are the initial sites to become excited [22, 32]. In Fig. 2 we show the time evolution of the global measure of entanglement given by Eq. (6) when the initial state <sup>1</sup> is site 1 or 6, for two temperatures: 77K and 300K <sup>2</sup>. The inset to this graph also includes the trace of the single excitation density

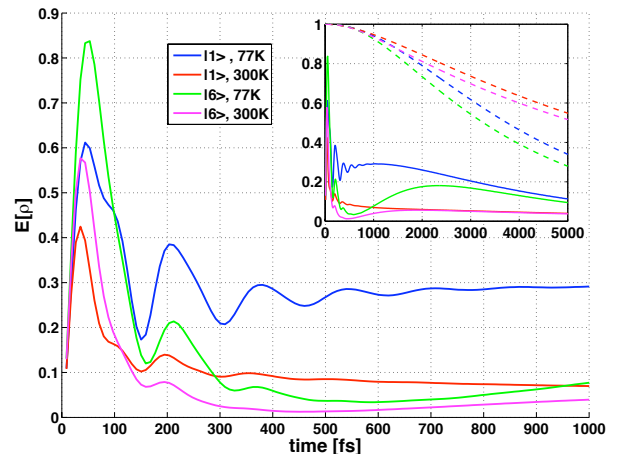


FIG. 2: Time evolution of the global entanglement measure given in Eq. (6) for the two initial states  $|1\rangle$  and  $|6\rangle$ , at low ( $T=77 \text{ K}$ ) and high ( $T=300 \text{ K}$ ) temperatures. The inset shows the long-time evolution of the same quantities, together with the trace of the single excitation density matrix as dashed curves (identical color coding).

matrix to show the total population in the single excitation subspace. A general feature of the global entanglement measure in all the scenarios depicted in Fig. 2 is that its value rises rapidly for short times and then after  $\sim 20 - 50 \text{ fs}$  decays with varying amounts of oscillation. An explanation for this behavior is that entanglement increases rapidly for short times due to quick delocalization of the excitation caused by large 1-2 and 5-6 site coupling terms in the FMO complex Hamiltonian. Then, as the excitation begins exploring other sites, the global entanglement decreases due to incoherent transport and rapid dephasing. For both initial conditions and temperatures, there is finite entanglement in the system up to 5ps. At 77K there is initially more entanglement in the complex when the excitation begins at site  $|6\rangle$ , but this entanglement decays quickly and at long times there is more entanglement in the system for initial state  $|1\rangle$ . At 300K the short time behavior is qualitatively similar to the low temperature case. At long times, however, the initial state dependence of the global entanglement is suppressed in contrast to the low temperature case.

A peculiarity of Fig. 2 for initial state  $|6\rangle$  is that the global entanglement decreases rapidly to almost zero but then increases again after  $\sim 600 \text{ fs}$ . To understand this behavior, and to further elucidate the structure of entanglement in the FMO monomer under realistic conditions, we examine pairwise entanglement in the system, as measured by the bipartite concurrence between two sites:  $C_{ij} = 2|\rho_{ij}|$  for any two sites  $i, j$ . Figures 3 and 4 show the time evolution of pairwise concurrence when the initial state is  $|1\rangle$  and  $|6\rangle$ , respectively, at both 77K and 300K. For clarity, only concurrence curves for the most entangled sites are shown, but it should be noted that

<sup>1</sup> Here, by “initial state” we mean the state of the FMO complex immediately after the arrival of excitation energy from the LHC chlorosome.

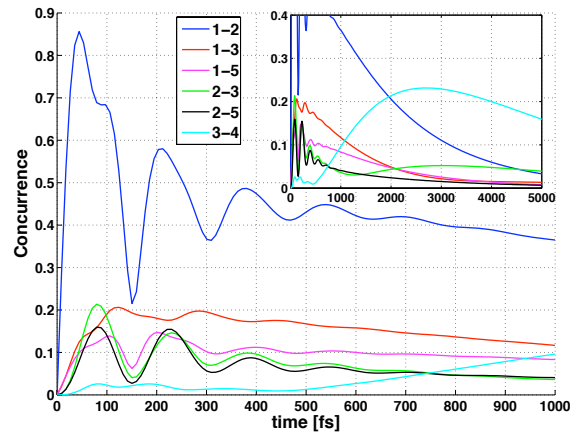
<sup>2</sup> We perform simulations for dynamics at 77K because the ultrafast spectroscopy experiments that probe LHCs are typically performed at this temperature.

there is finite bipartite entanglement between almost all chromophores, especially for short time scales.

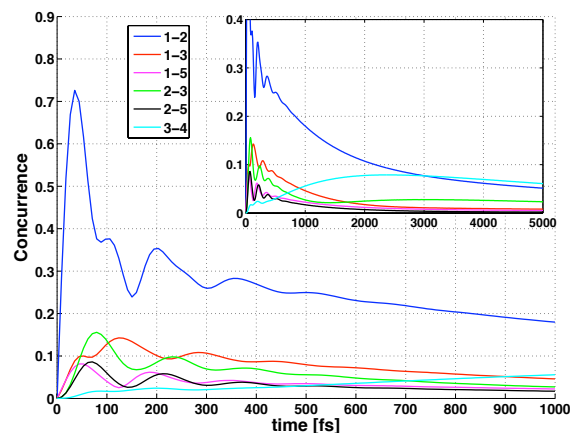
When the initial excitation is on site 1, as shown in Fig. 3, the bipartite entanglement in the complex is primarily between sites 1-2, 1-3, 2-3, and 3-4. Most of this bipartite entanglement is between pairs of moderately strongly coupled chromophores that form dimers and hence have large amounts of coherence. However, a surprising aspect of the short time behavior is that there is considerable concurrence between non-nearest-neighbor sites, as indicated by the 1-5 and 1-3 and 2-5 curves. Perhaps most strikingly, there is a large amount of entanglement within 1ps between chromophores 1 and 3, which are almost the furthest apart in the FMO complex (separated by  $\sim 28\text{\AA}$ ), and are very weakly coupled. This long-range entanglement is mediated by chromophores connecting these sites, and is a sign of multipartite entanglement in the system. At 77K bipartite entanglement persists for greater than 5ps, and seems limited only by the energy trapping rate – essentially there is non-negligible entanglement as long as the excitation has not been trapped by the reaction center. Bipartite entanglement persists for long periods of time at 300K also, but it diminishes at a faster rate compared to low temperatures. However, note that at short times ( $< 600\text{ps}$ ) temperature has little effect on the amount of bipartite entanglement in the system – qualitatively, the concurrence is scaled by  $\sim 3/4$  when the temperature is increased from 77K to 300K.

When the initial excitation is on site 6, as shown in Fig. 4, bipartite entanglement exists between several chromophores at short times; there is non-negligible entanglement between any two of the sites: 4, 5, 6 and 7. Note that not all of these are dimerized chromophores with large couplings. Furthermore, the presence of finite entanglement across any bipartite partition of the sites 4, 5, 6 and 7 indicates that the FMO complex contains genuine multipartite distributed entanglement within  $\sim 600\text{fs}$ .

Returning to Fig. 2, we now see that this characterization of bipartite entanglement aids in the interpretation of the dynamics of the global entanglement measure. In that figure it is seen that when the initial state is  $|6\rangle$ ,  $E[\rho]$  decreases to almost zero and then increases again after  $\sim 600\text{fs}$ . From examining the dissection of bipartite entanglement in the system (Fig. 4) one can surmise that this is because the excitation is rapidly transported and localized to sites 3 and 4 within  $\sim 600\text{fs}$ , resulting in the initial damping of multipartite entanglement. However, the coupling of sites 3 and 4 then delocalizes the excitation across these sites (forming the lowest energy exciton) and increases entanglement in the system, before reaction center trapping eventually leads to decay of population, coherence and entanglement. Traces of the site populations as a function of time support this conclusion [30]. This phenomenon of decreasing then increasing entanglement does not occur when the initial state is  $|1\rangle$  because: (i) the transport of the excitation to sites 3 and 4 occurs much more slowly and thus entanglement between sites



(a) Low temperature (77K)

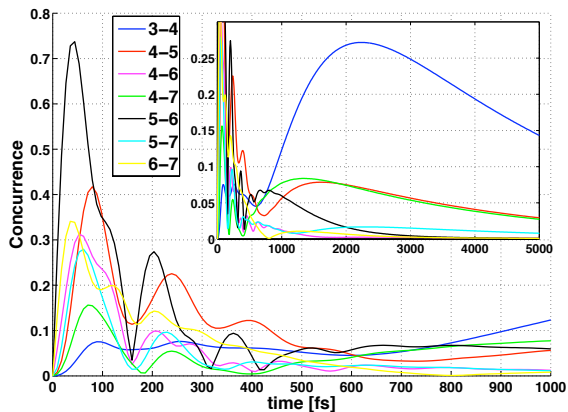


(b) High temperature (300K)

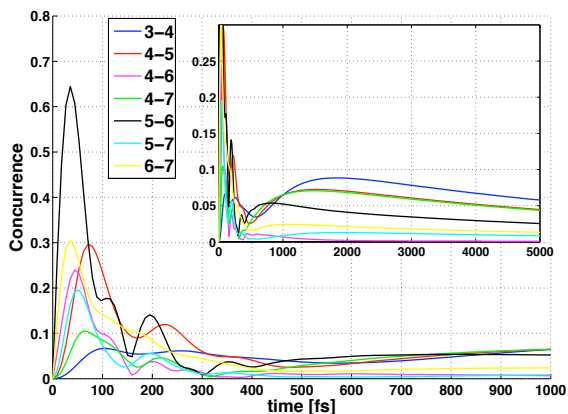
FIG. 3: Time evolution of the concurrence measure of bipartite site entanglement,  $C_{ij} = 2|\rho_{ij}|^2$ , when the initial state is an excitation localized on site 1. Only curves for the most entangled chromophores are shown. Inset shows the long time behavior.

1 and 2 persists for longer times, and (ii) when the lowest energy exciton is reached and the excitation energy is delocalized across sites 3 and 4, the increase in entanglement this creates is compensated by the decrease in entanglement created by the loss of coherence between sites 1 and 2. Again, traces of population dynamics in this system support this interpretation [30].

To summarize, realistic simulations of FMO dynamics indicate that considerable multipartite entanglement is present in the FMO complex at timescales of  $\sim 5\text{ps}$  at 77K and  $\sim 2\text{ps}$  at 300K. The initial excitation in FMO under natural conditions is localized on site 1 or 6, and we compared the entanglement generated by dynamics under both initial states. In both cases there is multipartite entanglement between all sites involved in excitation transport (mainly sites 1, 2, 3, and 4 when the initial state  $|1\rangle$ , and mainly sites 3, 4, 5, 6, and 7 when



(a) Low temperature (77K)



(b) High temperature (300K)

FIG. 4: Time evolution of the concurrence measure of bipartite site entanglement,  $C_{ij} = 2|\rho_{ij}|^2$ , when the initial state is an excitation localized on site 6. Only curves for the most entangled chromophores are shown. Inset shows the long time behavior.

the initial state is  $|6\rangle$ .

Finally, we compare the predictions for entanglement in the FMO complex made from this analysis of simulations with realistic incorporation of protein reorganization dynamics [29], to predictions made from analysis of more standard simulations based on the Markovian Redfield equation. Figure 5 shows the time evolution of the global entanglement measure  $E[\rho]$  when the initial state is  $|1\rangle$  at 300K, for three models of FMO dynamics: the I-F model, the Redfield model with the secular approximation (which is equivalent to the Lindblad formulation of Markovian dynamics [33, 34]), and the full Redfield equation without any additional approximations. On the whole, the full Redfield model overestimates, while the Redfield model with the secular approximation underestimates entanglement in the system. Notice that neither of these approximate Redfield models capture the oscillations in global entanglement that our theory predicts

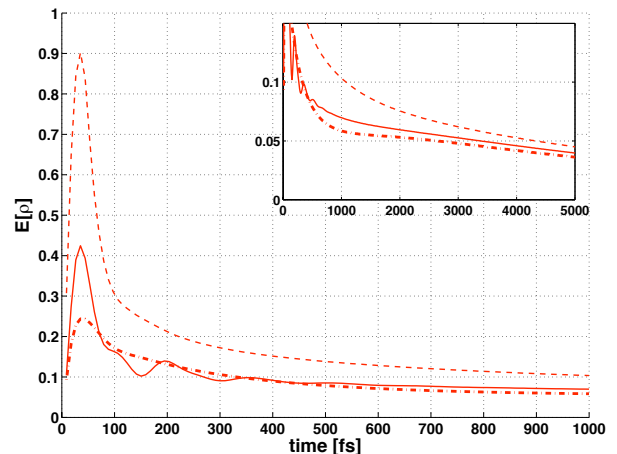


FIG. 5: Comparison of time dependence of predicted global entanglement in the FMO complex for three different simulation models of the excitation dynamics. Solid curve: evolution of the entanglement measure  $E[\rho]$  when the dynamics is generated with the I-F model of Ref. [29], as in Figures 2 – 4. Dashed curve: evolution of  $E[\rho]$  when the dynamics is generated by the full Redfield equation. Dash-dotted curve: evolution of  $E[\rho]$  with dynamics generated by the Redfield equation with the secular approximation. Inset shows the long time behavior of the same quantities.

with simulations according to the I-F equations. This is due to the fact that, unlike the I-F model, neither Redfield model realistically accounts for the phonon relaxation dynamics that occur at timescales comparable to excitation dynamics.

#### IV. DISCUSSION

The last section presented numerical evidence for the existence of entanglement in the FMO complex for picosecond timescales – essentially until the excitation is trapped by the reaction center. This is remarkable in a biological or disordered system at physiological temperature. It illustrates that non-equilibrium multipartite entanglement can exist for relatively long times, even in highly decoherent environments. While the length scales over which entanglement was shown to persist were small, we expect that such long-lived, non-equilibrium entanglement will nevertheless also be present in larger light harvesting antenna complexes, such as LH1 and LH2 in purple bacteria. This is because they contain the key necessary ingredient; namely, moderately strongly coupled chromophores that can lead to significant coherent delocalization of electronic excitations. In fact such delocalization has been observed and studied recently in connection to superradiance and ultrafast radiative decays in molecular aggregates [13, 35]. In larger light harvesting antennae it may also be possible to take advantage of the ability to create and support multiple excitations

in order to access a richer variety of entangled states.

We emphasize that our prediction of entanglement in the FMO complex is experimentally verifiable because the timescales on which the entanglement exists can readily be probed using non-linear femtosecond spectroscopy techniques. The ability to perform quantum state tomography on light harvesting complexes is not currently possible, but techniques are under development that will allow one to extract individual density matrix elements. The primary obstacle to this task is the determination of excitonic transition dipoles in the complex because the spectroscopy signals representing elements of the density matrix are scaled by the magnitude of these dipoles. It has recently been demonstrated that polarization-dependent two-dimensional spectroscopy is capable of determining these dipole moments [27], and hence the dynamical estimation of density matrix elements is within reach. The entanglement witness,  $\mathcal{W}$ , simplifies the experimental verification of entanglement since it implies that monitoring a small subset of site basis coherences (for example, the ones expected to be the largest in magnitude) is sufficient for detecting entanglement.

We now comment on the role of entanglement in the functioning of LHCs. It is well known in the chemical physics community that the dipole couplings present in densely packed molecular aggregates such as LHCs can lead to coherence between sites (e.g. Refs.[13, 14] and references therein). In fact, it is typical to model excited electronic states of such aggregates as Frenkel excitons that are delocalized coherently across several chromophores. These delocalized Frenkel exciton states represent entangled states of the chromophores and usually have lifetimes on the order of picoseconds. Following several precise characterizations of the structure of light harvesting complexes, the effects of inter-site electronic coherence on macroscopic properties of these complexes – e.g. absorption spectra, exciton transfer efficiency, radiative decay – have been studied. For example, in Refs. [36, 37, 38] it is shown that the excitation energy transfer rates seen in the LH2 complex of purple bacteria can be effectively explained by inter-site coherence. Similarly, Ref. [39] showed that inter-site coherence improves the uniformity and robustness of excitation energy transfer in LH2 in the presence of disorder. These studies, and others, present convincing evidence for the beneficial role of quantum coherence in excitation transport in light harvesting complexes [40]. And while entanglement in these systems is a by-product of this quantum coherence – since as discussed in this work, in the presence of coherence entanglement naturally exists for states in the single excitation subspace – it is however not clear whether it has a significant role in the functioning of light harvesting complexes. The non-local correlations of chromophoric electronic states that entanglement embodies are unlikely to impact excitation transport, the main function of LHCs. It is more plausible that entanglement exists merely as a consequence of the critical electronic coherence and the

resulting excitation delocalization.

Even if it does not play a significant role in the light harvesting functioning of LHCs, the existence of entanglement in these systems has important practical implications due to the technological applications of entangled states. For example, the presence of entanglement in LHCs sets the stage for investigating the applicability of entanglement-enhanced precision measurement [41] in biological systems. Ultra-precise quantum metrology enabled by the use of entangled states has been demonstrated using photons and ions, and these engineered systems have been used to measure frequencies and phases to unprecedented precision [42, 43]. The application of ideas from entanglement-enhanced metrology to the improved measurement of biological properties in these naturally robust quantum coherent systems is likely to be fruitful. Within this context, note that the observed enhanced radiative decay of delocalized (and hence entangled) electronic excitation states of LH1 and LH2 [13] is a result of the fact that those entangled states are more sensitive probes of the environment than separable states.

In addition to precision metrology, densely packed molecular aggregates such as LHCs have potential for constructing naturally robust quantum devices. For example, ultra-fast quantum state transfer facilitated by excitation migration along engineered or self-assembled chromophoric arrays could be a possible realization of the “quantum wires” that are much sought after in quantum technology. Entanglement between sub-units in such an array is essential for high-fidelity quantum transport, and as our study shows, such entanglement is possible in molecular aggregate structures even at room temperature. This conclusion is reinforced by recent studies at room temperature that have presented evidence for delocalization of excitations along molecular wires formed by self-assembling  $J$ -aggregates [44]. Integration of such molecular aggregates with solid-state devices (e.g. cavities [45]) opens up the possibility of engineering controllable quantum coherent soft matter structures that can be used to distribute or quantum states or entanglement. It should be noted that the control overhead for quantum state transfer in such wires is not overly prohibitive – it has been shown that the only requirement for high fidelity state transfer in *randomly* coupled linear chains is complete control (e.g optical addressability) over the end points of the linear chain [46].

Finally, we also point out that the close resemblance of the coherent dynamics of LHCs to quantum walks suggests that these systems might be useful for the study of quantum-walk-enhanced computational algorithms (e.g. [47, 48, 49, 50]). Prior work in this area has focused on computational speed-up attained from using quantum walks on idealized, non-decoherent graphs [51]. Further study is required to determine whether quantum walks on non-symmetric graphs in the presence of decoherence (the ones that LHC dynamics resemble) still present sufficient speed-up and computational advantage to be of interest.

We conclude by returning to the foundational significance of entanglement – it represents a uniquely quantum form of strong correlation between physical systems. The identification of entanglement, which was referred to by Schrödinger as “*the characteristic trait of quantum mechanics, the one that enforces its entire departure from classical lines of thought*” [52], in a biological system under natural functioning conditions further expands the field of physical systems for which non-trivial and uniquely quantum signatures become manifest.

**Acknowledgements** We are grateful to Yuan-Chung Cheng, Jahan Dawlaty and Vlatko Vedral for useful con-

versations. This material is based upon work supported by DARPA under Award No. N66001-09-1-2026. This work was supported by the Director, Office of Science, Office of Basic Energy Sciences, of the U.S. Department of Energy under Contract No. DE-AC02-05CH11231 and by the Chemical Sciences, Geosciences and Biosciences Division, Office of Basic Energy Sciences, U.S. Department of Energy under contract DE-AC03-76SF000098. A.I. appreciates the support of the Japan Society for the Promotion of Science (JSPS) Postdoctoral Fellowship for Research Abroad.

- 
- [1] E. Schrödinger. *Die gegenwärtige situation in der quantenmechanik*. Naturwissenschaften, **23**, 807 (1935).
- [2] A. Einstein, B. Podolsky, N. Rosen. *Can quantum-mechanical description of physical reality be considered complete*. Phys. Rev., **47**, 777 (1935).
- [3] R. Horodecki, P. Horodecki, M. Horodecki, K. Horodecki. *Quantum entanglement* (2007).
- [4] L. Amico, R. Fazio, A. Osterloh, V. Vedral. *Entanglement in many-body systems*. Rev. Mod. Phys., **80**, 517 (2008).
- [5] V. Vedral. *Quantifying entanglement in macroscopic systems*. Nature, **453**, 1004 (2008).
- [6] V. Vedral. *Entanglement production in non-equilibrium thermodynamics*. J. Phys.: Conf. Ser., **143**, 012010 (2007).
- [7] L. Quiroga, F. J. Rodriguez, M. E. Ramirez, R. Paris. *Nonequilibrium thermal entanglement*. Phys. Rev. A, **75**, 032308 (2007).
- [8] J. Cai, S. Popescu, H. J. Briegel. *Dynamic entanglement in oscillating molecules* (2008). arXiv:0809.4906 [quant-ph].
- [9] G. S. Engel, T. R. Calhoun, E. L. Read, T.-K. Ahn, T. Mancal, Y.-C. Cheng, R. E. Blankenship, G. R. Fleming. *Evidence for wavelike energy transfer through quantum coherence in photosynthetic systems*. Nature, **446**, 782 (2007).
- [10] H. Lee, Y.-C. Cheng, G. R. Fleming. *Coherence dynamics in photosynthesis: protein protection of excitonic coherence*. Science, **316**, 1462 (2007).
- [11] E. Collini, G. D. Scholes. *Coherent intrachain energy migration in a conjugated polymer at room temperature*. Science, **323**, 369 (2009).
- [12] R. E. Blankenship. *Molecular mechanisms of photosynthesis*. Wiley-Blackwell (2002).
- [13] R. Monshouwer, M. Abrahamsson, F. van Mourik, R. van Grondelle. *Superradiance and exciton delocalization in bacterial photosynthetic light-harvesting systems*. J. Phys. Chem. B, **101**, 7241 (1997).
- [14] H. van Amerongen, L. Valkunas, R. van Grondelle. *Photosynthetic excitons*. World Scientific (2000).
- [15] S. Hill, W. K. Wootters. *Entanglement of a pair of quantum bits*. Phys. Rev. Lett., **78**, 5022 (1997).
- [16] M. Horodecki, P. Horodecki, R. Horodecki. *Separability of mixed states: necessary and sufficient conditions*. Phys. Lett. A, **223**, 1 (1996).
- [17] A. Peres. *Separability criterion for density matrices*. Phys. Rev. Lett., **77**, 1413 (1996).
- [18] V. Vedral, M. B. Plenio. *Entanglement measures and purification procedures*. Phys. Rev. A, **57**, 1619 (1998).
- [19] V. Vedral. *The role of relative entropy in quantum information theory*. Rev. Mod. Phys., **74**, 197 (2002).
- [20] R. E. Fenna, B. W. Matthews. *Chlorophyll arrangement in a bacteriochlorophyll protein from Chlorobium limicola*. Nature, **258**, 573 (1975).
- [21] A. Camara-Artigas, R. E. Blankenship, J. P. Allen. *The structure of the FMO protein from Chlorobium tepidum at 2.2 Å resolution*. Photosynth. Res., **75**, 49 (2003).
- [22] J. Adolphs, T. Renger. *How proteins trigger excitation energy transfer in the FMO complex of green sulfur bacteria*. Biophysical J., **91**, 2778 (2006).
- [23] A. G. Redfield. *On the theory of relaxation processes*. IBM J. Res. Dev., **1**, 19 (1957).
- [24] V. May, O. Kuhn. *Charge and energy transfer dynamics in molecular systems*. Wiley-VCH (2004).
- [25] T. Brixner, J. Stenger, H. M. Vaswani, M. Cho, R. E. Blankenship, G. R. Fleming. *Two-dimensional spectroscopy of electronic couplings in photosynthesis*. Nature, **434**, 625 (2005).
- [26] M. Cho, H. M. Vaswani, T. Brixner, J. Stegner, G. R. Fleming. *Exciton analysis in 2D electronic spectroscopy*. J. Phys. Chem. B, **109**, 10542 (2005).
- [27] E. L. Read, G. S. Schlau-Cohen, G. S. Engel, J. Wen, R. E. Blankenship, G. R. Fleming. *Visualization of excitonic structure in the Fenna-Matthews-Olson photosynthetic complex by polarization-dependent two-dimensional electronic spectroscopy*. Biophysical J., **95**, 847 (2008).
- [28] A. Ishizaki, G. R. Fleming. *On the adequacy of the redfield equation and related approaches to the study of quantum dynamics in electronic energy transfer* (2009). J. Chem. Phys. (In press).
- [29] A. Ishizaki, G. R. Fleming. *Unified treatment of quantum coherent and incoherent hopping dynamics in electronic energy transfer: reduced hierarchy equations approach* (2009). J. Chem. Phys. (In press).
- [30] A. Ishizaki, G. R. Fleming. *Quantum coherence in photosynthetic systems at physiological temperature: Numerical investigation* (2009). (In preparation).
- [31] T. Förster. *Zwischenmolekulare energiewanderung und fluoreszenz*. Ann. Phys. (Leipzig), **2**, 55 (1948).
- [32] J. Wen, H. Zhang, M. L. Gross, R. E. Blankenship. *Membrane orientation of the FMO antenna pro-*

- tein from *Chlorobaculum tepidum* as determined by mass spectrometry-based footprinting. *Proc. Nat. Acad. Sc.*, **106**, 6134 (2009).
- [33] G. Lindblad. *On the generators of quantum dynamical semigroups*. *Comm. Math. Phys.*, **48**, 119 (1976).
- [34] H.-P. Breuer, F. Petruccione. *The theory of open quantum systems*. Oxford University Press (2002).
- [35] T. Meier, Y. Zhao, V. Chernyak, S. Mukamel. *Polarons, localization, and excitonic coherence in superradiance of biological antenna complexes*. *J. Chem. Phys.*, **107**, 3876 (1997).
- [36] K. Mukai, S. Abe, H. Sumi. *Theory of rapid excitation-energy transfer from B800 to optically-forbidden exciton states of B850 in the antenna system LH2 of photosynthetic purple bacteria*. *J. Phys. Chem. B*, **103**, 6096 (1999).
- [37] G. D. Scholes, G. R. Fleming. *On the mechanism of light harvesting in photosynthetic purple bacteria: B800 to B850 energy transfer*. *J. Phys. Chem. B*, **104**, 1854 (2000).
- [38] S. Jang, M. D. Newton, R. J. Silbey. *Multichromophoric forster resonance energy transfer*. *Phys. Rev. Lett.*, **92**, 218301 (2004).
- [39] Y.-C. Cheng, R. J. Silbey. *Coherence in the B800 ring of purple bacteria LH2*. *Phys. Rev. Lett.*, **96**, 028103 (2006).
- [40] H. Sumi. *Bacterial photosynthesis begins with quantum-mechanical coherence*. *Chem. Record*, **1**, 480 (2001).
- [41] V. Giovannetti, S. Lloyd, L. Maccone. *Quantum-enhanced measurements: Beating the standard quantum limit*. *Science*, **306**, 1330 (2004).
- [42] C. F. Roos, M. Chwalla, K. Kim, M. Riebe, R. Blatt. *'Designer atoms' for quantum metrology*. *Nature*, **443**, 316 (2006).
- [43] T. Nagata, R. Okamoto, J. L. O'Brien, K. Sasaki, S. Takeuchi. *Beating the standard quantum limit with four-entangled photons*. *Science*, **316**, 726 (2007).
- [44] P. G. Lagoudakis, M. M. de Souza, F. Schindler, J. M. Lupton, J. Feldmann, J. Wenus, D. G. Lidzey. *Experimental evidence for exciton scaling effects in self-assembled molecular wires*. *Phys. Rev. Lett.*, **93**, 257401 (2004).
- [45] J. R. Tischler, M. S. Bradley, Q. Zhang, T. Atay, A. Nurmikko, V. Bulovic. *Solid state cavity QED: strong coupling in organic thin films*. *Org. Electronics*, **8**, 94 (2007).
- [46] D. Burgarth, S. Bose. *Perfect quantum state transfer with randomly coupled quantum chains*. *New J. Phys.*, **7**, 135 (2005).
- [47] A. M. Childs, R. Cleve, E. Deotto, E. Farhi, S. Gutmann, D. A. Spielman. *Exponential algorithmic speedup by quantum walk*. In *Proc. 35th ACM Symposium on Theory of Computing*, page 59. ACM (2003).
- [48] N. Shenvi, J. Kempe, K. B. Whaley. *Quantum random-walk search algorithm*. *Phys. Rev. A*, **67**, 052307 (2003).
- [49] A. M. Childs, J. Goldstone. *Spatial search by quantum walk*. *Phys. Rev. A*, **70**, 022314 (2004).
- [50] A. Ambainis. *Quantum walk algorithm for element distinctness*. *SIAM J. Comp.*, **37**, 210 (2007).
- [51] A. Ambainis. *Quantum walks and their algorithmic applications*. *Int. J. Quantum Inf.*, **1**, 507 (2003).
- [52] E. Schrödinger. *Discussion of probability relations between separated systems*. *Proc. Cambridge Phil. Soc.*, **31**, 555 (1935).